PAN ARCHIVES OF ACOUSTICS
Vol. 43, No. 3, pp. 447–453 (2018)

DOI: 10.24425/123916

Using Empirical Mode Decomposition of Backscattered Ultrasound Signal Power Spectrum for Assessment of Tissue Compression

Michał BYRA, Janusz WÓJCIK, Andrzej NOWICKI

Department of Ultrasound
Institute of Fundamental Technological Research
Polish Academy of Sciences
Pawińskiego 5B, 02-106 Warsaw, Poland; e-mail: mbyra@ippt.pan.pl

(*received March 1, 2018; accepted June 15, 2018*)

Quantitative ultrasound has been widely used for tissue characterization. In this paper we propose a new approach for tissue compression assessment. The proposed method employs the relation between the tissue scatterers' local spatial distribution and the resulting frequency power spectrum of the backscattered ultrasonic signal. We show that due to spatial distribution of the scatterers, the power spectrum exhibits characteristic variations. These variations can be extracted using the empirical mode decomposition and analyzed. Validation of our approach is performed by simulations and *in-vitro* experiments using a tissue sample under compression. The scatterers in the compressed tissue sample approach each other and consequently, the power spectrum of the backscattered signal is modified. We present how to assess this phenomenon with our method. The proposed in this paper approach is general and may provide useful information on tissue scattering properties.

Keywords: tissue characterization; tissue compression; quantitative ultrasound; empirical mode decomposition; signal analysis.

1. Introduction

Ultrasound imaging has been widely used for soft tissue characterization. The images of tissue scanned with ultrasounds are obtained through the reconstruction of radio-frequency (RF) echo-signals backscattered in the tissue under examination. Various quantitative ultrasound (QUS) methods were proposed to extract tissue properties based on RF data (Mamou, Oelze, 2013). QUS includes the assessment of backscatter properties, attenuation coefficients, and envelope statistics (Oelze, Mamou, 2016).

Tissue is commonly modeled as a matrix of scattering source centers that are fundamentally divided into coherent and diffusive ones (Zhou *et al.*, 2017). Coherent scatterers are by definition positioned periodically within investigated tissue while spatial distribution of diffusive scatterers is considered to be random. Specific spatial distribution of scatterers results in different backscattering and characteristic speckle patterns observed in B-mode ultrasound images. For example, periodically positioned scatterers are expected to produce specific oscillations in the RF signal power spectrum. These oscillations can be analyzed in various ways, e.g. using the cepstrum method (Lizzi *et al.*, 1981).

Spatial distribution of scatterers within tissue under compression is modified. In this paper we propose a new spectral based method for tissue compression assessment. The proposed method, called the SPD (RF Signal Power spectrum mode Decomposition), offers some insight into the relation between the scatterers spatial distribution and the backscattered echo spectrum. We show that the power spectrum oscillations are generally related to the distances between the scatterers. This observation leads to the concept of intrinsic mode functions (IMFs). We show that the RF signal spectrum is composed of IMFs related to tissue microstructure. Next, it is depicted how the empirical mode decomposition (EMD) can be applied to extract power spectrum oscillations. Finally, we describe how to use these spectrum oscillations for tissue compression assessment.

This paper is organized in the following way. Our method is described in the next section. We show theoretically how the power spectrum variations can be

related to the spatial distribution of scatterers. Next, it is described how to extract those variations using the EMD. Moreover, the approach is illustrated using numerical simulations. Next, a simple *in-vitro* experiment is performed using an uncompressed and compressed tissue sample scanned with a linear array transducer. The scatterers in the sample of squeezed tissue approach each other and consequently, the power spectrum of the backscattered signal is modified. It is described how these fluctuations of the backscattered spectra can be determined using our method. Finally, the results are presented and discussed.

2. Materials and methods

2.1. Method description

The concept of the SPD relies on the scatterer point model. The echo backscattered from a single scatterer (denoted by index k) is expected to be a scaled copy of the incident ultrasonic pulse, which can be expressed in the following way:

$$f_k(t) = r_k p(t - t_k), \tag{1}$$

where r_k is the k-th scatterer reflectivity and $p(t - t_k)$ refers to the incident pulse being scattered at the k-th point and recorded with time delay $t_k = 2d_k/c$, d_k is the distance from the k-th scatterer to the transmitting/receiving transducer, c is the speed of sound. Assuming single scattering approximation and allowing linear interference only, the backscattered echo from the cluster of scatterers can be written as:

$$f(t) = \sum_{k=1}^{L} r_k p(t - t_k), \tag{2}$$

where L is the number of all scatterers in medium or investigated region of interest (ROI). For a stochastic medium r_k and t_k are random variables. Although this model is one-dimensional and simplified, it provides a good description of ultrasonic echoes obtained with linear array transducers used in US imaging (SHUNG, 1993).

Equation (2) is usually separated into two sums corresponding to diffuse-like and periodic scatterers (ZHOU *et al.*, 2017). Here, however, we follow a different approach. First of all, the Fourier transform of Eq. (2) is:

$$F(\omega) = P(\omega) \sum_{k=1}^{L} r_k \mathrm{e}^{i\omega t_k}. \tag{3}$$

Next, the power spectrum of $f(t)$ can be expressed in the following form (WÓJCIK *et al.*, 2016):

$$|F(\omega)|^2 = |P(\omega)|^2 \left[\boldsymbol{R}^2 + \sum_{k=1}^{L} \sum_{l=1}^{L-1} 2r_{k,l} \cos(\omega t_{k,l}) \right], \tag{4}$$

where

$$\boldsymbol{R}^2 = \sum_{k=1}^{L} r_k^2, \qquad r_{k,l} = r_k r_l, \qquad t_{k,l} = t_k - t_l.$$

Moreover, we can write:

$$\begin{aligned} I(\omega) &= |F(\omega)|^2 = |P(\omega)|^2 Q(\omega) \\ &= |P(\omega)|^2 \left(Q_0(\omega) + \widetilde{Q}(\omega) \right) \\ &= I_0(\omega) + \widetilde{I}(\omega), \end{aligned} \tag{5}$$

where

$$Q_0(\omega) = \boldsymbol{R}^2,$$

$$\widetilde{Q}(\omega) = \sum_{k=1}^{L} \sum_{l=1}^{L-1} 2r_{k,l} \cos(\omega t_{k,l}),$$

$$I_0(\omega) = |P(\omega)|^2 Q_0(\omega),$$

$$\widetilde{I}(\omega) = |P(\omega)|^2 \widetilde{Q}(\omega).$$

The $Q(\omega)$ component is related to the reflective properties of the medium and it includes the oscillatory content of the spectrum $\widetilde{Q}(\omega)$ that results from periodically spaced scattering sources. The power spectrum oscillates in the frequency domain and the rate of these oscillations is related to the distribution of inter-distances $t_{k,l}$ between pairs of scatterers weighted by $r_{k,l}$. For clarity, we express the inter-distances in time domain, however the relation holds $t_{k,l} = 2d_{k,l}/c$ and $d_{k,l} = d_k - d_l$ establishing a direct link between the time and space domain.

Before we continue lets remind the concept of the IMF. A single IMF can be written as (DAUBECHIES *et al.*, 2011):

$$u(t) = U(t) \cos(\varphi(t)), \tag{6}$$

where the phase $\varphi(t)$ is non-decreasing and the envelope $U(t)$ is positive. This relation holds in the Fourier domain as well if we consider variable ω as the primary one:

$$u(\omega) = U(\omega) \cos(\varphi(\omega)), \tag{7}$$

Relation between Eq. (7) and the power spectrum is straightforward. $\widetilde{Q}(\omega)$ is composed of IMFs which phase depends on the scatterer inter-distances $t_{k,l}$, $\varphi(\omega) = \cos(t_{k,l}\omega)$. Moreover, the envelope of each IMF is constant and equal to $r_{k,l}$. Next, using the Wiener-Khinchin theorem we can write the inverse Fourier transform of $Q(\omega)$ to obtain the "medium autocorrelation" function:

$$q(t) = q_0 + \widetilde{q}(t) = \boldsymbol{R}^2 \delta(0) + \sum_{k=1}^{L} \sum_{l=1}^{L-1} 2r_{k,l} \delta(\omega t_{k,l}), \tag{8}$$

where $\delta(\cdot)$ is the Dirac delta function. In the case of constant $r_{k,l}$, $\widetilde{q}(t)$ can be considered as the distribution

of inter-distances between scatterers in the medium (or two elements clusters distribution). For L scatterers the summation in Eq. (8) goes over the number of all possible inter-distances equal to $N = L(L-1)/2$. We can conclude from Eq. (8) that the medium autocorrelation function for larger t should be affected by inter-distances of higher values.

The resulting received backscattered echo is equal to the convolution of the medium autocorrelation function $q(t)$ and $\gamma(t)$ that represents the scanning pulse $p(t)$ autocorrelation:

$$W(t) = \gamma(t) * q(t), \tag{9}$$

where $*$ refers to convolution operator in respect to time. Similarly to $Q(\omega)$, we can divide $W(t)$ into $W_0(t)$ and variable part $\widetilde{W}(t)$. Despite the blurring effect we present below that the scatterers' spatial distribution still can be assessed using RF data. It can be done by extracting power spectrum oscillations. We illustrate the concept of the SPD with numerical simulations. Figure 1a shows the distribution of scatterers' reflectivities and positions, and Fig. 1b displays the corresponding $\widetilde{q}(t)$ function from Eq. (8). Additionally $|W(t)|$ is presented in Fig. 1c. Reflectivities and positions are expressed in mm and were sampled uniformly from [0.75, 1.25] and [0, 20], respectively. We used only 20 scatterers for clarity which corresponds to $N = 190$. The emitted pulse consisted of 2 cycle sine wave with a triangular envelope, center frequency was equal to 6 MHz. The speed of sound was constant and equal to 1540 m/s. Calculations were performed using Matlab (the MathWorks, Inc).

The aim of the SPD is to extract power spectrum oscillations and to provide quantitative analysis. For this task we use the EMD which has been widely used in signal analysis for IMF extraction. The EMD (the sifting process) can be described in the following way (HUANG *et al.*, 1998):

1) Find all the local extremes in the signal.
2) Connect all the local maxima to create the upper envelope.

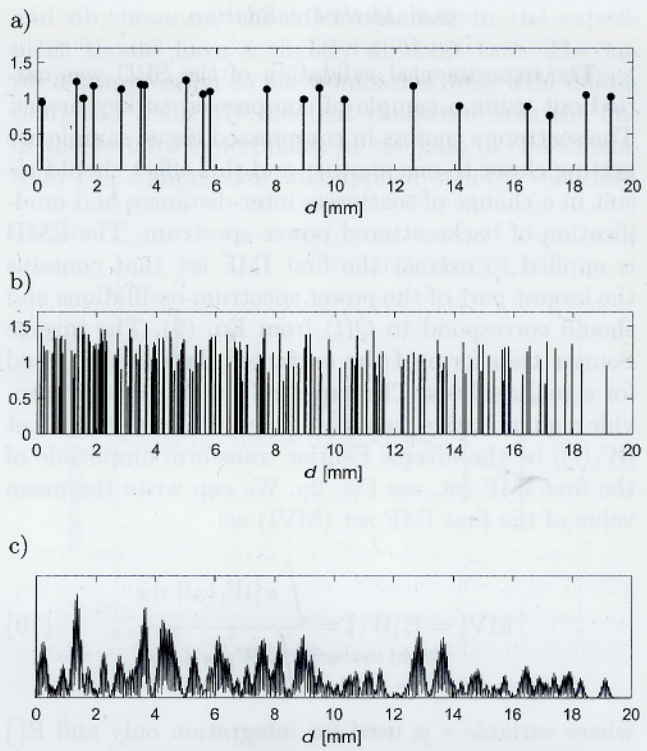

Fig. 1. The signal autocorrelation is related to the distribution of the scatterers: a) distribution of scatterers along a line, b) $\widetilde{q}(t)$ from Eq. (8), c) $|W(d)|$ from Eq. (9).

3) Connect all the local minima to create the lower envelope.
4) Calculate the mean envelope (signal trend).
5) Subtract the mean envelope from the signal to obtain the first IMF.
6) Repeat the above procedure to extract the second IMF from the first.

Result of one iteration of the above sifting process applied to the power spectrum is illustrated in Fig. 2b. EMD extracts IMFs that contain the most of the power spectrum oscillations.

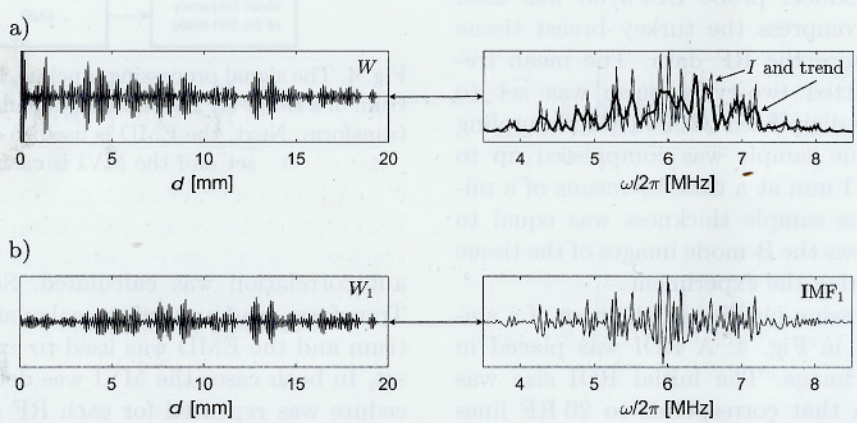

Fig. 2. Illustration of the proposed method. The oscillations of the signal power spectrum are extracted using EMD inverse Fourier transform (a) applied to the signal power spectrum and the first IMF (b).

2.2. Method validation

The experimental validation of the SPD was carried out using a sample of compressed turkey breast. The scatterers centers in compressed tissue sample are getting closer to one another and this effect should result in a change of scatterers inter-distances and modification of backscattered power spectrum. The EMD is applied to extract the first IMF set that contains the largest part of the power spectrum oscillations and should correspond to $\widetilde{Q}(t)$ from Eq. (5). The inverse Fourier transform of the extracted data is then used for signal analysis. The expected value is used to provide a quantitative measure of spectrum variations. Let $|W_1(t)|$ be the inverse Fourier transform amplitude of the first IMF set, see Fig. 2a. We can write the mean value of the first IMF set (MVI) as:

$$\mathrm{MVI} = \mathrm{E}\left[W_1\right] = \frac{\int s\,|W_1(s)|\,\mathrm{d}s}{\int |W_1(s)|\,\mathrm{d}s}, \tag{10}$$

where variable s is used for integration only and E[·] refers to the expectation operator.

The motivation beyond Eq. (10) is simple. In the compressed tissue the scatterers' inter-distances $t_{k,l}$ decrease and the distribution $\widetilde{q}(t)$ in Eq. (8) should experience a shift. One may consider an unrealistic scenario where the scatterers are compressed to a single point and the oscillations disappear.

Two experiments were carried out. First, the tissue sample was compressed in a quasi-static way and next, a simulation was conducted to examine the predictions on MVI behavior stated above. Simulation parameters were selected to imitate the *in-vitro* experiment as close as possible.

2.3. Experiment

The Ultrasonix SonixTouch Research scanner (Ultrasonix, British Columbia, Canada) equipped with a linear array transducer probe L14-5/38 was used simultaneously to compress the turkey breast tissue sample and to acquire the RF data. The mean frequency of the emitted two-cycle pulse was set to 6 MHz. Echoes were digitalized with 40 MHz sampling frequency. The tissue sample was compressed up to 7 mm with steps of 1 mm at a time by means of a micrometric table. The sample thickness was equal to 50 mm. Figure 3 shows the B-mode images of the tissue sample acquired during the experiment.

The signal processing pipeline in the case of a single image is shown in Fig. 4. A ROI was placed in the middle of the image. The initial ROI size was equal to 20×5 mm that corresponds to 20 RF lines with 1000 RF samples each. Within the ROI each RF line was extracted and processed separately. First, the autocorrelation was calculated. Second, the Fourier Transform was applied to calculate the power spectrum and the EMD was used to extract the first IMF set. In both cases the MVI was determined. This procedure was repeated for each RF signal line. Results were averaged and the standard deviation was calculated.

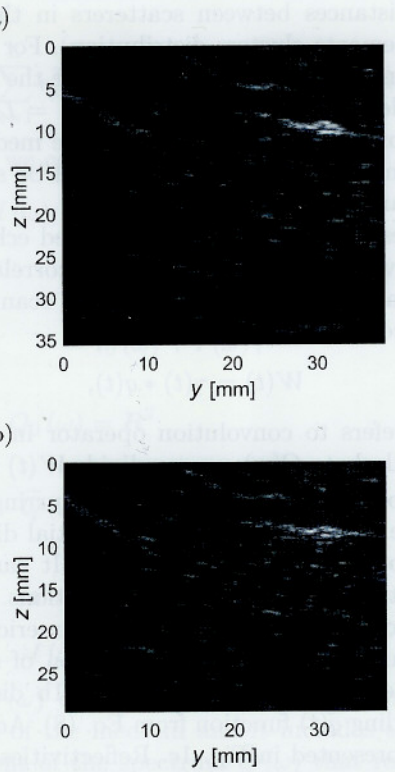

Fig. 3. The tissue sample: a) before the compression, b) after compression, displacement of 7 mm.

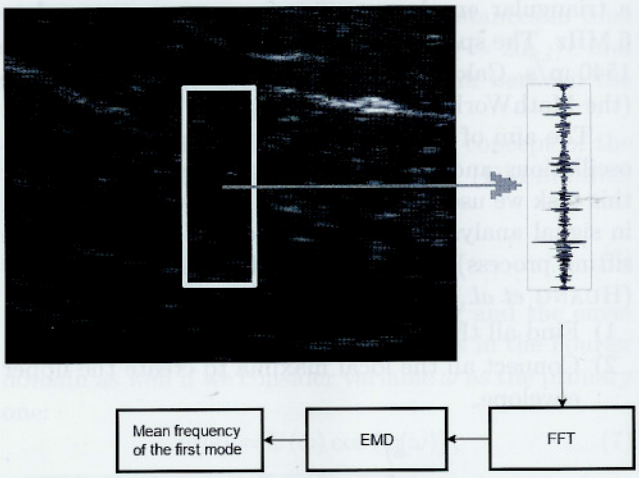

Fig. 4. The signal processing pipeline. First, the power spectrum of a single RF signal line is calculated with the Fourier transform. Next, the EMD is used to extract the first IMF set and the MVI is calculated.

2.4. Simulation

The aim of the simulation was to model tissue compression in the similar way as in the *in-vitro* experiment. To accomplish this, we used the approach described in the Method concept subsection. However, now a single line was generated based on 60 scatterers spread along the line to avoid blank spaces in the RF signal. To imitate the compression inside the ROI, 20 RF lines were simulated and each line was shortened up to 2.8 mm with a step of 0.4 mm. Mean values and standard deviations of MVIs were calculated.

3. Results

3.1. Simulation

The autocorrelation function (from Fig. 2) modified due to the shortening of the scanning line by 2.8 mm after compression is shown in Fig. 5. Figure 6a shows the normalized MVI as a function of applied compression. MVI values were normalized in respect to MVI calculated for uncompressed data. Linear regression was used to model the MVI-compression relation. We obtained high value of the coefficient of determination ($R^2 > 0.99$) indicating strong linear dependence.

3.2. Experiment

MVIs obtained in the *in-vitro* experiment are depicted in Fig. 6b. The R^2 parameter calculated for the method utilizing first IMF set was equal 0.95.

4. Discussion

Due to applied compression the scatterers are more densely distributed within the investigated tissue sample. This phenomenon is illustrated in Fig. 6a. As the tissue sample is compressed, the power spectrum becomes less variable and the normalized MVI decreases. This result is in a good agreement with the numerical simulation shown in Fig. 6b. Comparing Fig. 6a and 6b, however, the MVI obtained in the experiment should have a slightly different rate. The applied compression in the simulation (one axis dilatation) had a slightly different character than the one in the *in-vitro* experiment. In the case of the simulation, the compression was applied strictly vertically,

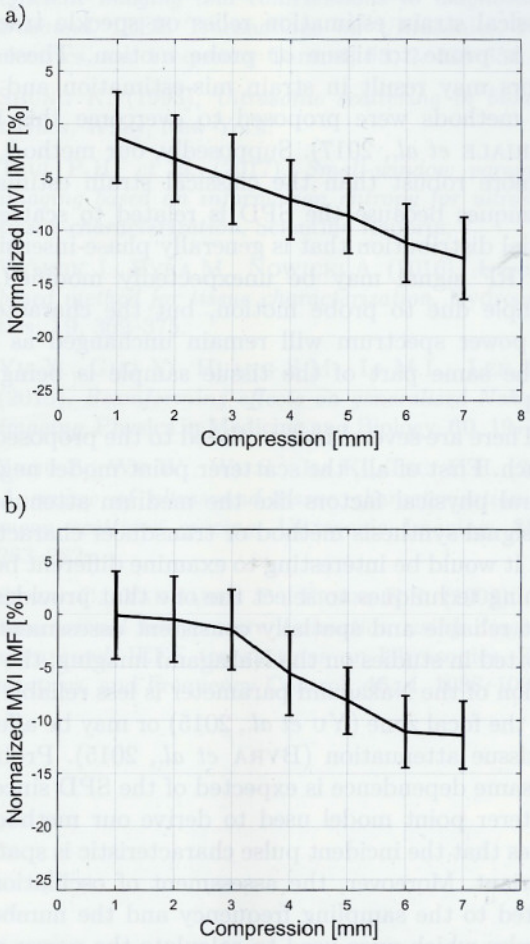

Fig. 6. MVI for the first IMF set in the case of the: a) numerical experiment, and b) the *in-vitro* experiment. Compression results in decrease of the MVI.

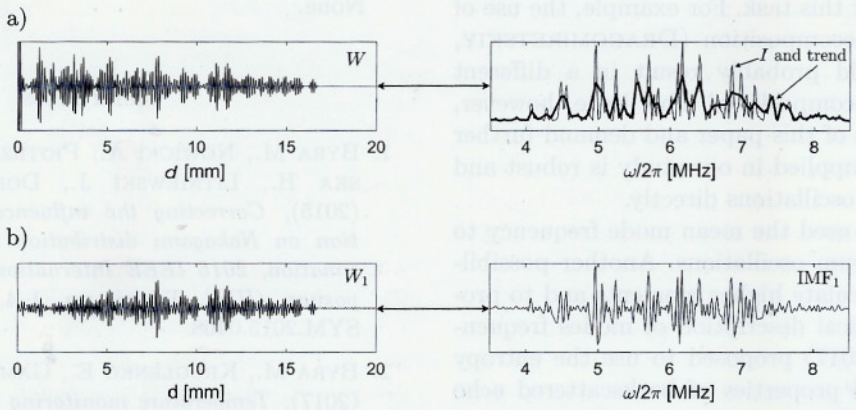

Fig. 5. Impact of compression on the autocorrelation function decompositions (a) from Fig. 2a and on the EMD power spectrum decomposition (b) from Fig. 2b. Compression modifies the frequency content of the signal.

but in the tissue sample also a lateral shift could appear. For both these deformation types, however, the distances between the scatterers should be modified.

Presumably, the SPD can be used for tissue deformation monitoring. The MVI estimation may be a more practical method of strain assessment, for example in the case of heart wall (DANDEL *et al.*, 2009). Classical strain estimation relies on speckle tracking and is prone to tissue or probe motion. These two factors may result in strain mis-estimation and several methods were proposed to overcome this issue (CURIALE *et al.*, 2017). Supposedly, our method may be more robust than the classical strain estimation techniques because the SPD is related to scatterers' spatial distribution that is generally phase-insensitive. The RF signal may be unexpectedly modified, for example due to probe motion, but the character of the power spectrum will remain unchanged as long as the same part of the tissue sample is being imaged.

There are several issues related to the proposed approach. First of all, the scatterer point model neglects several physical factors like the medium attenuation, RF signal synthesis method or transducer characteristics. It would be interesting to examine different beamforming techniques to select the one that provides the most reliable and spatially consistent assessment. As reported in studies on the Nakagami imaging, the estimation of the Nakagami parameter is less reliable outside the focal zone (YU *et al.*, 2015) or may be affected by tissue attenuation (BYRA *et al.*, 2015). Probably the same dependence is expected of the SPD since the scatterer point model used to derive our method assumes that the incident pulse characteristic is spatially invariant. Moreover, the assessment of oscillations is related to the sampling frequency and the number of samples which were used to calculate the power spectrum. These values should be high enough to provide good resolution in the Fourier domain.

Another issue is the uniqueness of the proposed approach. We used the EMD to extract power spectrum oscillations. However, there are other methods that could be applied for this task. For example, the use of variational mode decomposition (DRAGOMIRETSKIY, ZOSSO, 2014) would probably result in a different power spectrum decomposition. This issue, however, is beyond the scope of this paper and demand further studies. The EMD applied in our study is robust and extracts significant oscillations directly.

In this work we used the mean mode frequency to assess power spectrum oscillations. Another possibility would be to calculate higher moments and to provide a more statistical description of modes frequencies. TSUI *et al.* (2017) proposed to use the entropy to assess statistical properties of backscattered echo amplitudes. Although the context was different, in our case the entropy can be applied to determine the level of randomness in scatterers spatial distribution instead of using the MVI.

As to future applications, we consider our method as a general QUS technique which can be applied to various problems related to tissue characterization. For example, it can be used for temperature monitoring (GHOSHAL *et al.*, 2016; BYRA *et al.*, 2017). As the temperature is increased in the tissue, for example by high intensity ultrasound technique, the speed of sound is modified (SIMON *et al.*, 1998). This phenomenon results in a change of scatterers' axial distribution (according to the formula $t = 2d/c$) which supposedly can be assessed with the proposed approach.

5. Conclusions

In this paper we described a new approach to compression assessment. The STD is based on extraction of RF signal power spectrum oscillations which contain the information on scatterers' spatial distribution within investigated tissue. The method was examined numerically and validated by means of an *in-vitro* experiment using tissue sample before and after compression. We have shown that the compression influences power spectrum oscillations and that it can be effectively monitored with our method.

The STD can be perceived as a QUS technique. In the future we would like to compare various methods of oscillations extraction and to investigate the impact of beamforming technique on estimated quantities. Moreover, we plan to apply our method to issues which have been already addressed by other QUS techniques.

Acknowledgment

This work was supported by the National Science Center Grant Number UMO-2014/13/B/ST7/01271.

Conflict of interest statement

None.

References

1. BYRA M., NOWICKI A., PIOTRZKOWSKA-WRÓBLEWSKA H., LITNIEWSKI J., DOBRUCH-SOBCZAK K. (2015), *Correcting the influence of tissue attenuation on Nakagami distribution shape parameter estimation, 2015 IEEE International Ultrasonics Symposium (IUS)*, Taipei, pp. 1–4, doi: 10.1109/ULTSYM.2015.0408.

2. BYRA M., KRUGLENKO E., GAMBIN B., NOWICKI A. (2017), *Temperature monitoring during focused ultrasound treatment by means of the homodyned K distribution*, Acta Physica Polonica A, **131**, 6, 1525–1528.

3. Curiale A.H., Vegas-Sanchez-Ferrero G., Aja-Fernandez S. (2017), *Influence of ultrasound speckle tracking strategies for motion and strain estimation*, Medical Image Analysis, **32**, 184–200.

4. Dandel M., Lehmkuhl H., Knosalla C., Suramelashvili N., Hetzer R. (2009), *Strain and strain rate imaging by echocardiography-basic concepts and clinical applicability*, Current Cardiology Reviews, **5**, 2, 133–148.

5. Daubechies I., Lu J., Wu H.T. (2011), *Synchrosqueezed wavelet transforms: An empirical mode decomposition-like tool*, Applied and Computational Harmonic Analysis, **30**, 2, 243–261.

6. Dragomiretskiy K., Zosso D. (2014), *Variational mode decomposition*, IEEE Transactions on Signal Processing, **62**, 531–544.

7. Ghoshal G., Kemmerer J.P., Karunakaran C., Miller R.J., Oelze M. (2016), *Quantitative ultrasound for monitoring high-intensity focused ultrasound treatment in vivo*, IEEE Transactions on Ultrasonics, Ferroelectrics, and Frequency Control, **63**, 9, 1234–1242.

8. Huang N.E. *et al.* (1998), *The empirical mode decomposition and the Hilbert spectrum for nonlinear and non-stationary time series analysis*, Proceedings of the Royal Society A: Mathematical, Physical and Engineering Sciences, **454**, 1971, 903–995.

9. Lizzi F., Feleppa E., Jaremko N. (1981), *Liver-tissue characterization by digital spectrum and cepstrum analysis*, [in:] *1981 Ultrasonics Symposium*, pp. 575–578.

10. Mamou J., Oelze M. (2013), *Quantitative ultrasound in soft tissues*, Springer, Netherlands.

11. Oelze M., Mamou J. (2016), *Review of quantitative ultrasound: envelope statistics and backscatter coefficient imaging and contributions to diagnostic ultrasound*, IEEE Transactions on Ultrasonics, Ferroelectrics, and Frequency Control, **63**, 2, 336–351.

12. Shung K. (1993), *Ultrasonic scattering in biological tissues*, Wiley, New York.

13. Tsui P.H. *et al.* (2017), *Small-window parametric imaging based on information entropy for ultrasound tissue characterization*, Scientific Reports, 7.

14. Wójcik J., Byra M., Nowicki A. (2016), *A spectral-based method for tissue characterization*, Hydroacoustics, **19**, 369–375.

15. Yu X., Guo Y., Huang S.M., Li M.L., Lee W.N. (2015), *Beamforming effects on generalized Nakagami imaging*, Physics in Medicine and Biology, **60**, 19, 7513.

16. Zhou Z., Wu W., Wu S., Jia K., Tsui P.H. (2017), *A review of ultrasound tissue characterization with mean scatterer spacing*, Ultrasonic Imaging, **39**, 5, 263–282.

17. Simon C., VanBaren P., Ebbini E.S. (1998), *Two-dimensional temperature estimation using diagnostic ultrasound*, IEEE transactions on Ultrasonics, Ferroelectrics, and Frequency Control, **45**, 4, 1088–1099.